Available online at www.sciencedirect.com

SCIENCE DIRECT®

Journal of the European Ceramic Society 24 (2004) 3593–3601

www.elsevier.com/locate/jeurceramsoc

A new glass–ceramic red pigment

Federica Bondioli[a,*], Tiziano Manfredini[a], Cristina Siligardi[a], Anna Maria Ferrari[b]

[a] *Dipartimento di Ingegneria dei Materiali e dell'Ambiente, Università di Modena e Reggio Emilia, Via Vignolese 905/a, Modena 41100, Italy*
[b] *Dipartimento di Scienza e Metodi dell'Ingegneria, Università di Modena e Reggio Emilia, Reggio Emilia 42100, Italy*

Received 19 September 2003; received in revised form 1 December 2003; accepted 7 December 2003

Abstract

Recently in the traditional ceramic industry there has been an increasing interest in the obtainment of inclusion pigments to stabilize at the firing temperature and towards the actions of molten glasses unstable cromophore such as hematite or cadmium sulphoselenide.
This work focuses on a new synthesis of hematite-zircon inclusion pigment obtained from sintering of non-conventional mixture of precursors. To this purpose a glass composition belonging to the Li_2O–ZrO_2–SiO_2 system that during the sintering/devetrification steps crystallizes zircon has been chosen. The employment of two different Fe precursors (oxide and goethite) have been also analyzed. Finally, a mechanism of pigment formation is proposed.

Keywords: Pigments; Glass–ceramics; Colour

1. Introduction

Inorganic natural and synthetic pigments produced and marketed as fine powders are an integral part of many decorative and protective coatings and are used for the mass coloration of many materials, including glazes, ceramic bodies, and porcelain enamels. In all these applications, pigments are dispersed (they do not dissolve) in the media, forming a heterogeneous mixture. In conclusion, powders used for coloring ceramics must show thermal and chemical stability at high temperature and must be inert to the action of molten glass (frits or sintering aids).

These requirements limit ceramic pigments to a very small number of refractory systems which are fully reacted and relatively inert to the matrix in which they are dispersed. This need for great chemical and thermal stability has dominated research and development in recent years.[1] In particular, the interest is directed to the development of inclusion pigments which make utilizable coloring substances suffering the industrial, thermal, and chemical conditions by occluding them in a stable glassy or crystalline matrix (heteromorphic pigments). Early works[2–4] report red- and orange-zircon pigments prepared by inclusion of some inorganic compounds (i.e. $Cd(S_xSe_{1-x})$) in the zircon network to obtain a pigment with sufficient chemical and thermal stability at the firing temperature.[5] According to the denomination proposed by Lavilla and Rincon,[5] this new family of pigments present the following characteristics: (a) they are composed of two or more different insoluble crystalline structures; (b) their behavior in the presence of glazes is like a unique chromatic unit from a pigmentation point of view: the color is not developed by the introduction of a colored ion into the matrix lattice or by the formation of a solid solution, but the crystals responsible for the color are small colored crystals occluded in the matrix during its sintering process. Among the systems studied,[6,7] hematite included in zircon (DCMA 14-44-5),[8] also known as "coral pink" pigment, is one of the zircon-based pigments, together with the vanadium zircon blue $(V,Zr)SiO_4$ and the praseodymium zircon yellow $(Pr,Zr)SiO_4$, market leader in high temperature applications for the whitewares industry. The traditional synthesis of this pigment consists in mixing different Fe precursors (Fe_2O_3, $FeSO_4$, or $FeO(OH)$) with zirconia, silica, and several mineralizers (mainly alkaline or alkaline earth halides) and subsequently firing the obtained mixture to temperatures such as 900 °C.[9] Both zircon formation and hematite crystallization and coarsening must occur simultaneously in order to guarantee efficient occlusion of the hematite and, therefore, a high color yield.[10] In this sense, the control methods of these two stages are fundamental to obtain the cromophore

---

[*] Corresponding author. Tel.: +39-05920-56242; fax: +39-05920-56243.
E-mail address: bondioli.federica@unimore.it (F. Bondioli).

0955-2219/$ – see front matter © 2004 Elsevier Ltd. All rights reserved.
doi:10.1016/j.jeurceramsoc.2003.12.017

particle grow in an appropriate way in location and size in the same range of temperatures, so that it can be trapped by the matrix particles in their sintering process. The choice of the appropriate mineralizer becomes particularly important.

This work focuses on the synthesis and characterization of hematite-zircon inclusion pigment obtained from a sintering process of a non-conventional mixture of precursors. To avoid the use of the mineralizer and to optimize the pigment, a glass composition belonging to the Li_2O–ZrO_2–SiO_2 has been chosen as starting powder. This composition melts at a relative low temperature and during the thermal treatment step zircon crystallizes. The employment of two different Fe precursors (oxide and goethite) have been analyzed. In particular, a mechanism of pigment formation is proposed.

2. Experimental procedure

2.1. Sample preparation

The glass composition studied in this work belongs to the Li_2O–ZrO_2–SiO_2 phase diagram (SiO_2 69 mol%, Li_2O 20 mol%, ZrO_2 11 mol%). The composition has been prepared by melting reagent grade raw materials: lithium carbonate (Li_2CO_3, 100%), zirconium silicate ($ZrSiO_4$, 100%), and quartz (SiO_2, 99.9%). Batch, previously dry milled, has been melted in an electrically heated furnace within Pt crucibles, following the heating cycle: from 20 to 500 °C at 5 °C/min, from 500 to 1500 °C at 10 °C/min, and finally 30 min of soaking time at the maximum temperature of 1500 °C. The melts have been quenched in water in order to obtain a frit. Glassy powders have been obtained by wet milling in water using a fast laboratory ball mill (300 ml) with spherical alumina grinding in a 1:1 solid/distilled water ratio for 30 min and successively drying.

In order to synthesize glass–ceramic pigments, two different iron precursors, goethite (FeOOH) and hematite (Fe_2O_3), have been added (10 wt.% of hematite) to the glassy powder by dry mixing. The powdered base glass and the mixtures have been pressed at 400 kg/m^2 in order to obtain pellets that have been sintered for 1 h at 600, 700, 800, 850, 900, and 1000 °C with a heating rate of 10 °C/min. Pellets have been powdered in an agata mortar in order to obtain the adequate grain size distribution for the successive characterizations.

2.2. Powder characterization

To investigate the structure and crystallinity of the samples, the raw materials and the glass–ceramic pigments have been analyzed with a computer-assisted X-ray (Cu Kα) powder diffractometer (Model PW3710, Philips Research Laboratories). The X-ray diffraction (XRD) patterns have been collected in a 2θ range of 10–70° at room temperature, with a scanning rate of 0.005°/s and a step size of 0.02°. The particle size distribution has been determined by using a laser light particle size analyzer (Model Analyzette22, Fritsch). The thermal behavior of the powders up to 1300 °C has been evaluated by differential thermal analysis (DTA) (Model DSC 404, Netzch) with a heating rate of 10°/min. The morphology and microstructure of the samples have been examined by scanning electron microscopy (SEM) (Model XL40, Philips Research Laboratories) equipped with a energy dispersion spectroscopy (EDS) equipment (EDAX, Philips Research Laboratories). Small pieces of the obtained materials have been mounted in epoxy resin and superficially polished down to 0.2 μm alumina paste. The resin surface has been successively coated with a thin film of Au/Pd.

To confirm the effective inclusion of the hematite in the glass–ceramic matrix, leaching test in boiling solutions of concentrated (36 wt.%) hydrochloric acid has been performed on glass–ceramic pigments. In particular, 1 cc of HCl has been added to 20 mg of powdered sample having a particle size between 25 and 38 μm and then heated at 50 °C for 5 min. After filtration, the leached solution containing the iron ion, has been analyzed by an atomic emission spectroscopy inductively coupled plasma (AES-ICP) (Model Liberty 200, VARIAN).

Color measurements have been performed by UV–Vis spectroscopy (model Lambda 19, Perkin-Elmer) using the CIELab method in order to obtain L^*, a^*, and b^* values.

2.3. Semi-industrial application

The optimized pigments have been tested as pigments for ceramic bodies in comparison to both an industrial synthetic coral pink pigment and a natural Grès de Thiviers. A ceramic body, having a typical composition of fine porcelain stoneware tile bodies, has been used for pigment application (SiO_2 70 wt.%, Me_2O 5 wt.%, MeO 1.5 wt.%, Al_2O_3 18 wt.%, Fe_2O_3 0.5 wt.%, TiO_2 0.5 wt.%, L.O.I. 3.6 wt.%). The pigments, added to the composition at 2 wt.%, have been wet mixed (35 wt.% of water) with the ceramic composition for 30 min in a blender-mixer and then dried. The dried powders have been humidified to a water content of 5.5 wt.% and pressed at 40 MPa to produce wires (40-mm diameter) tile. Compacts have been dried to constant weight at 105 °C and then fired in an industrial high speed roller kiln using a typical industrial cycle of ~50 min with a maximum temperature of 1220 °C. The cromophore role of the pigments has been studied on the fired samples by ultraviolet and visible spectrophotometer (model Lambda 19, Perkin-Elmer) using the CIELab method in order to obtain L^*, a^*, and b^* values.

3. Results and discussion

3.1. Raw materials characterization

The base glass is transparent and homogeneous; X-ray diffraction pattern shows the characteristic broad band of the amorphous phase and examination by SEM shows no evidence of unmelted or crystalline phases.

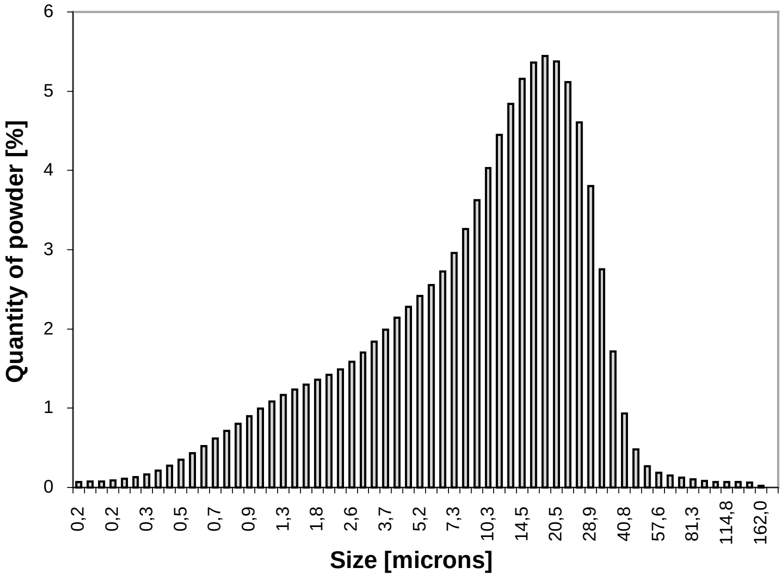

Fig. 1. Grain size distribution of the glassy phase after wet milling (30 min).

The powdered glass has a monomodal grain size distribution with an average size of 20 μm (Fig. 1). DTA thermogram of the studied composition (Fig. 2) presents the characteristic thermal event of a glassy phase: (a) an endothermic peak, T_g, at about 620 °C, corresponding to the glass transition temperature; (b) an exothermic event with a maximum at 920 °C, indicating the crystallization temperature, T_p; (c) an endothermic event with a minimum at 980 °C, indicating the melting temperature, T_m.

Fig. 3 reports the XRD pattern of the base glass heated at 800, 900, and 1000 °C. At 800 °C the sample is still amorphous while at 900 °C crystallized zircon ($ZrSiO_4$: ICDD 06-0266) as main phase and lithium–silicate, LS ($Li_2Si_2O_5$: ICDD 17-0447), lithium–zirconium–silicate, LZS ($Li_2ZrSi_6O_{15}$: ICDD 36-0049), and trydimite (SiO_2: ICDD 14-0260)[11] as minor phases. As the temperature is increased (1000 °C, Fig. 3c) the lithium–zirconium–silicate quantity increases while the trydimite quantity decreases.

SEM micrograph (Fig. 4) of 1000 °C heated sample evidences the presence of three different crystal forms immersed in a glass phase. In particular, it is possible to observe acicular crystals of zircon (as confirmed by EDS analysis), grey crystals of LZS, and some spherical shaped light grey crystal of LS.

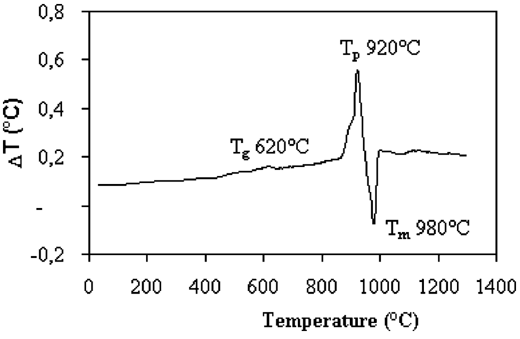

Fig. 2. DTA curve of the glass powdered sample.

These results show that the devetrification process of the chosen composition belonging to the Li_2O–ZrO_2–SiO_2 system starts at around 900 °C with a surface crystallization of zircon, lithium silicate, and trydimite. At higher temperature, lithium–zirconium–silicate also starts to crystallize while the endothermic event in the DTA curve at 980 °C could be assigned to the fusion of trydimite as underlined in the XRD patterns.

As regarding the two iron precursors used, the powders have a similar grain size distributions (Fig. 5) in order to avoid the grain size distribution variable effect on the sintering process.

3.2. Pigments characterization

When the iron precursor is added at the glassy powders, the thermal behavior is slightly different as confirmed by thermal analysis (DTA) and X-ray diffraction conducted on the sintered powders.

DTA thermograms of the studied mixtures (Fig. 6) present the characteristic thermal event of a glassy phase: independently from the iron precursor used, (a) an endothermic peak, T_g, at about 620 °C, corresponding to the glass transition temperature; (b) an exothermic broad peak with a maximum at 880 °C, indicating the crystallization temperature, T_p; (c) an endothermic event with a minimum at 950 °C, indicating the melting temperature, T_m. In particular, if goethite is used as iron precursor (Fig. 6), the DTA curve also presents an endothermic peak at 380 °C corresponding to the goethite dehydroxylation.

In particular, the T_p temperature of the mixed sample is lower than that of the glassy sample. This behavior is due

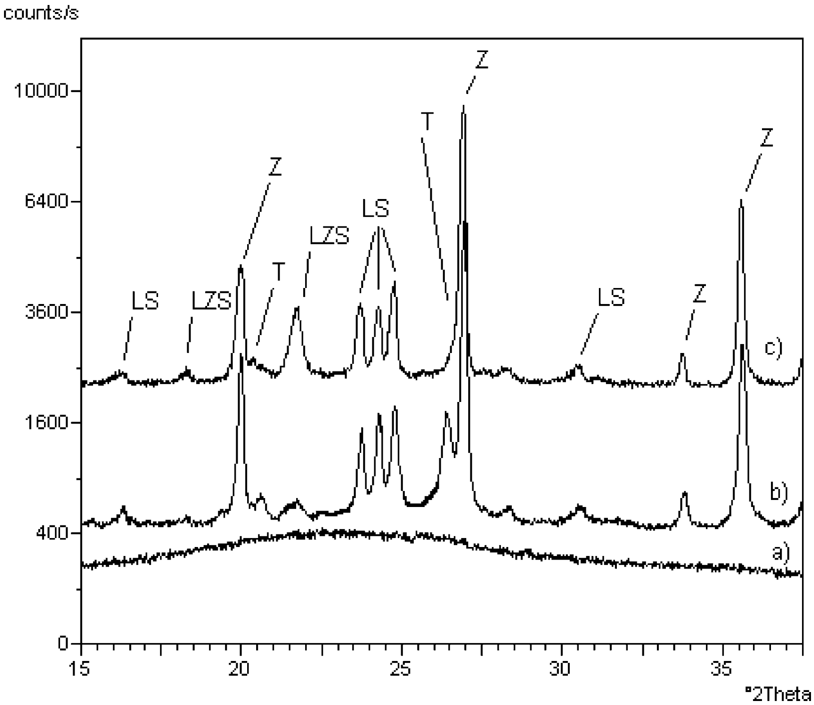

Fig. 3. Diffraction patterns of the glassy phase after thermal treatment at (a) 800 °C, (b) 900 °C, and (c) 1000 °C for 1 h (LS: $Li_2Si_2O_5$, LZS: $Li_2ZrSi_6O_{16}$, Z: $ZrSiO_4$, T: trydimite SiO_2).

to the fact that the presence of solid particles on the glass surface, as in this case Fe_2O_3 particles, produces preferential sites for surface nucleation.[12]

Fig. 7 reports the XRD pattern of the mixtures heated at 700, 800, 900, and 1000 °C. Up to 800 °C the only crystalline phase in the samples is, independently from the iron precursors used, hematite (Fig. 7a). At 800 °C (Fig. 7b) starts to crystallize trydimite (SiO_2: ICDD 14-0260), lithium silicate ($Li_2Si_2O_5$: ICDD 17-0447), and zircon ($ZrSiO_4$: ICDD) as minor phase. Starting from 850 °C (Fig. 7b) zircon becomes the main phase. Finally at 1000 °C (Fig. 7c) the only crystalline phases present in the sample are zircon and a lithium–zirconium–silicate phase ($Li_2ZrSi_6O_{15}$: ICDD 36-0049) while hematite, trydimite, and lithium

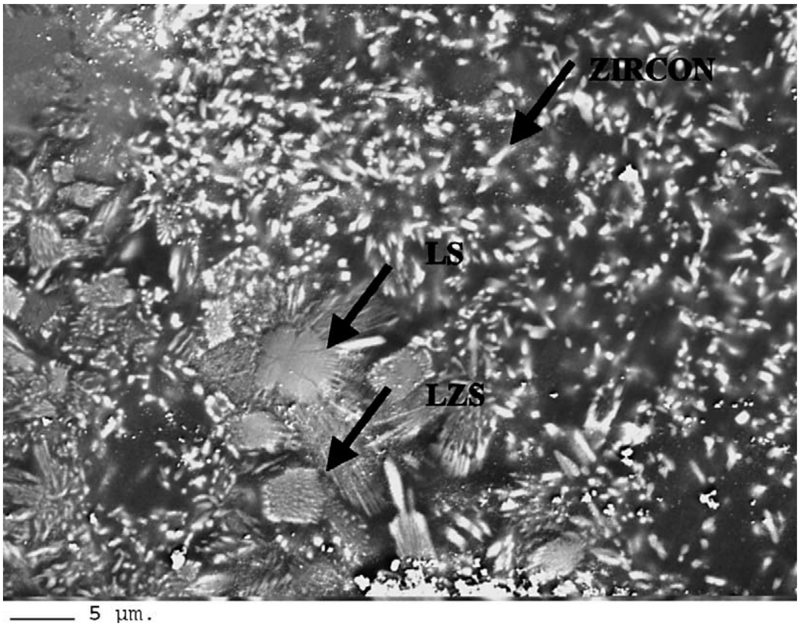

Fig. 4. SEM image of the sintered glassy powders (1 h at 1000 °C).

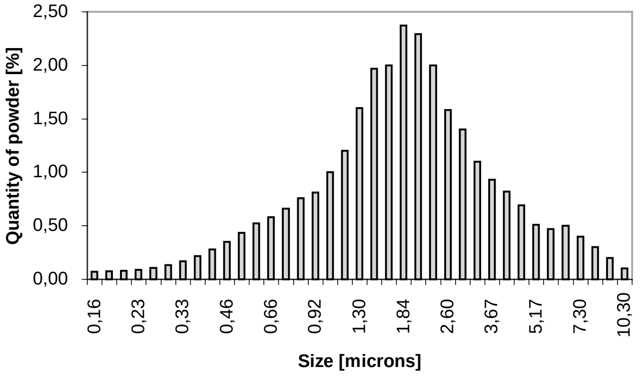

Fig. 5. Grain size distribution of iron precursors (in particular, Fe_2O_3 chosen as representative).

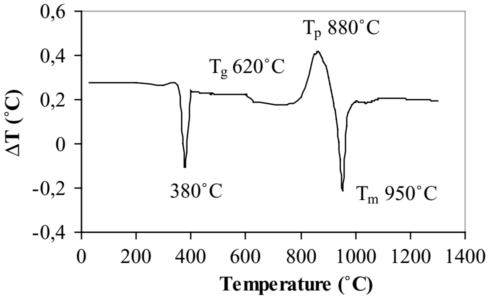

Fig. 6. DTA curves of the green mixtures obtained starting from goethite.

silicate phases disappear. The XRD analysis results are summarized in Table 1.

XRD analysis suggests, in agreement with DTA results, the faster thermal reactivity of the hematite containing samples with respect to the glassy composition. In particular, at 1000 °C not only trydimite but also lithium silicate melting is observed. This effect is probably due to the iron melting that decreases the viscosity of glass matrix producing a more reactive environment. This is also evidenced in the DTA curves that shows a decrease of the T_m temperature of the pigment mixture with respect to the base glass.

SEM micrographs (Fig. 8) of 800, 900, and 1000 °C heated sample evidence the microstructure of the heated sample. At 800 °C (Fig. 8a) small hematite crystals appear at the grain boundary of the amorphous phase. In this zone it is possible to underline a glassy phase crystallization. In particular, in Fig. 9 SEM micrograph obtained on the sintered pellet at 800 °C is reported with the X-ray maps of iron, zirconium, and silicium. At 900 °C (Fig. 8b) the crystallization of the glassy phase is completed; finally at 1000 °C (Fig. 8c) there is a further microstructure evolution with the formation, by melting, of a glassy phase in which two crystalline phases ($ZrSiO_4$ and $Li_2ZrSi_6O_{15}$ as confirmed by XRD) are dispersed and the acicular one is zircon. In this sense, the endothermal signal in the DTA

Table 1
XRD analysis results of the obtained pigments

Temperature (°C)	Main crystalline phases
600	**Glass**, **hematite**
700	**Glass**, **hematite**
800	**Tridymite**, **hematite**, $Li_2Si_2O_5$, zircon
850	**Zircon**, **hematite**, tridymite, $Li_2Si_2O_5$
900	**Zircon**, **hematite**, tridymite, $Li_2Si_2O_5$
1000	**Zircon**, $Li_2ZrSi_6O_{15}$, glass

In bold major phases.

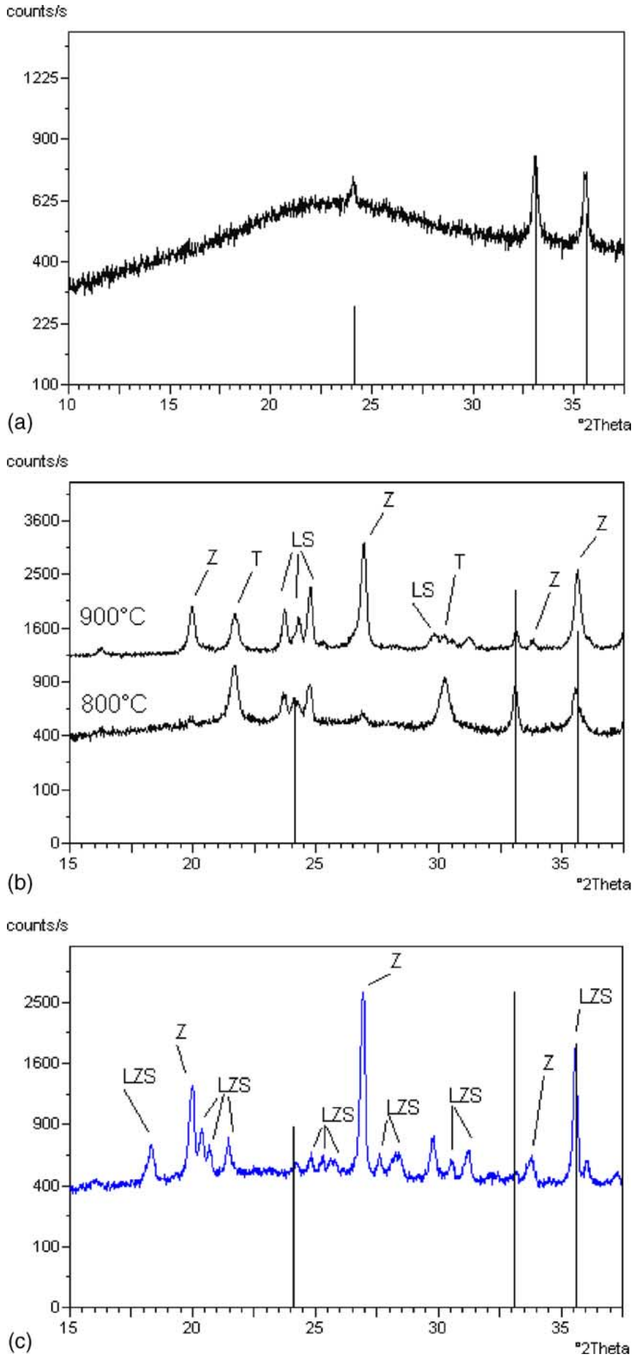

Fig. 7. Diffraction patterns of the mixture with goethite after sintering step for 1 h at (a) 700 °C, (b) 800 and 900 °C, (c) 1000 °C. Vertical lines correspond to Fe_2O_3 (ICDD 33-0664) (LS: $Li_2Si_2O_5$, LZS: $Li_2ZrSi_6O_{16}$, Z: $ZrSiO_4$, T: trydimite SiO_2).

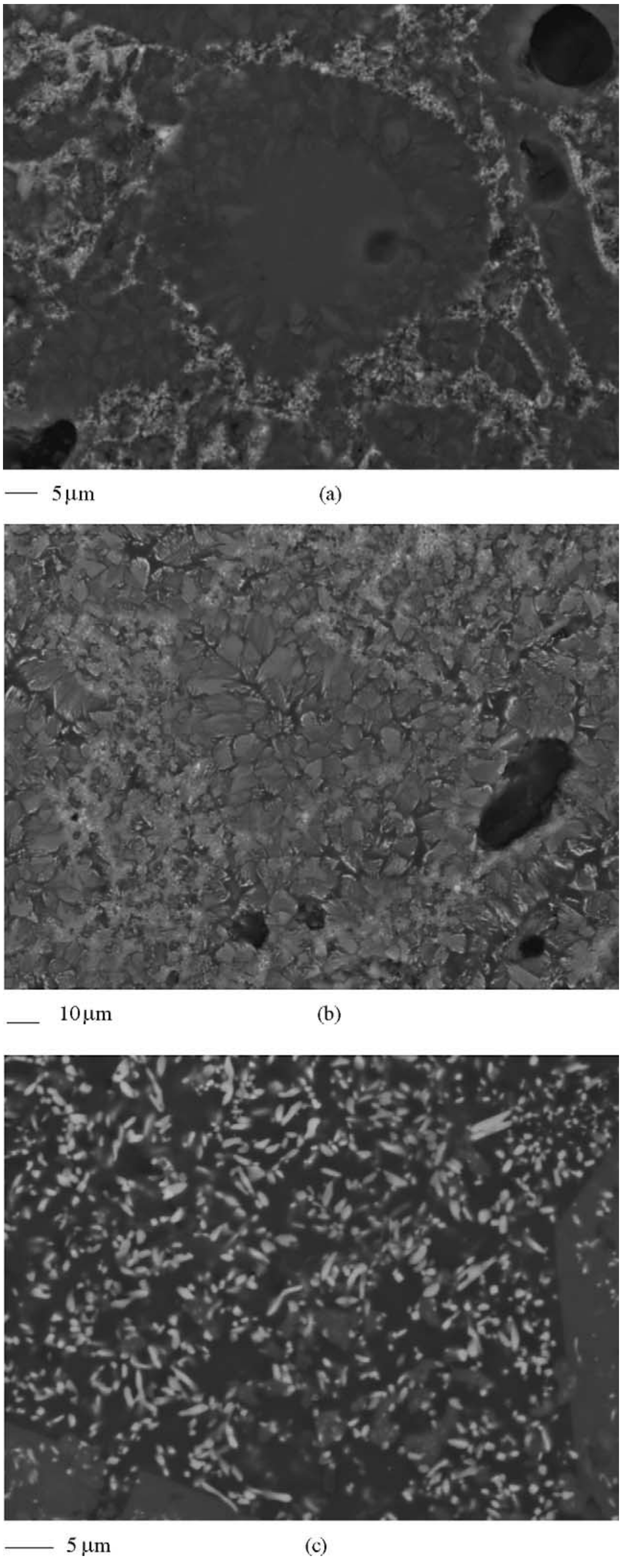

Fig. 8. SEM micrographs of sintered glass–ceramic pigment after thermal treatment at (a) 800 °C, (b) 900 °C, and (c) 1000 °C.

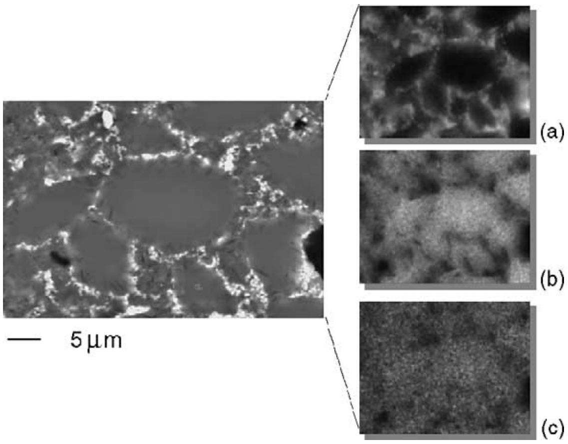

Fig. 9. SEM micrograph and X-ray maps of (a) iron, (b) silicium, and (c) zirconium for the 800 °C, 1 h sintered sample.

curves (Fig. 6) has to be associated to the LS and trydimite phases fusion in agreement with the value reported in literature. From EDS spectra (here not reported) iron seems to be present exclusively in the new formed amorphous phase.

From these data, the better temperature for the inclusion process seems to be 850–900 °C independently from the iron precursor used.

In particular, in Fig. 10, the SEM micrograph of a section of the 850 °C 1 h powders is reported. The powdered sample is prepared in epoxy resin and subsequently polished in order to obtain a section of the pigment grains. This preparation allows to verify as zircon crystals (white crystals) protect hematite ones (grey zone) as confirmed by EDS analysis.

In order to verify the inclusion efficiency as a function of both sintering temperature and type of iron precursors, leaching test has been performed. As free hematite is easily solubilized in boiling hydrochloric acid to form iron(III) soluble chloride, chemical attach may be considerably suitable to evaluate the hematite trapping into zircon crystals (Table 2). The obtained values indicate that the iron leached decreases with increasing the sintering temperature. The better occlusion seems to be reached starting from goethite for heating temperature of 850–900 °C (<2.5 ppm) even if the values of powders obtained starting from hematite are very close. At higher temperature, the iron release still decreases; this effect has to be correlated to the hematite dissolution

Table 2
Fe (ppm) leached of the samples treated at different temperature for 1 h

	Samples	
	LZS + Fe_2O_3	LZS + FeOOH
Green	10.6	14.7
600 (°C)	8.6	13.0
700 (°C)	7.1	7.8
800 (°C)	4.0	4.4
900 (°C)	2.6	2.1
1000 (°C)	1.1	0.4

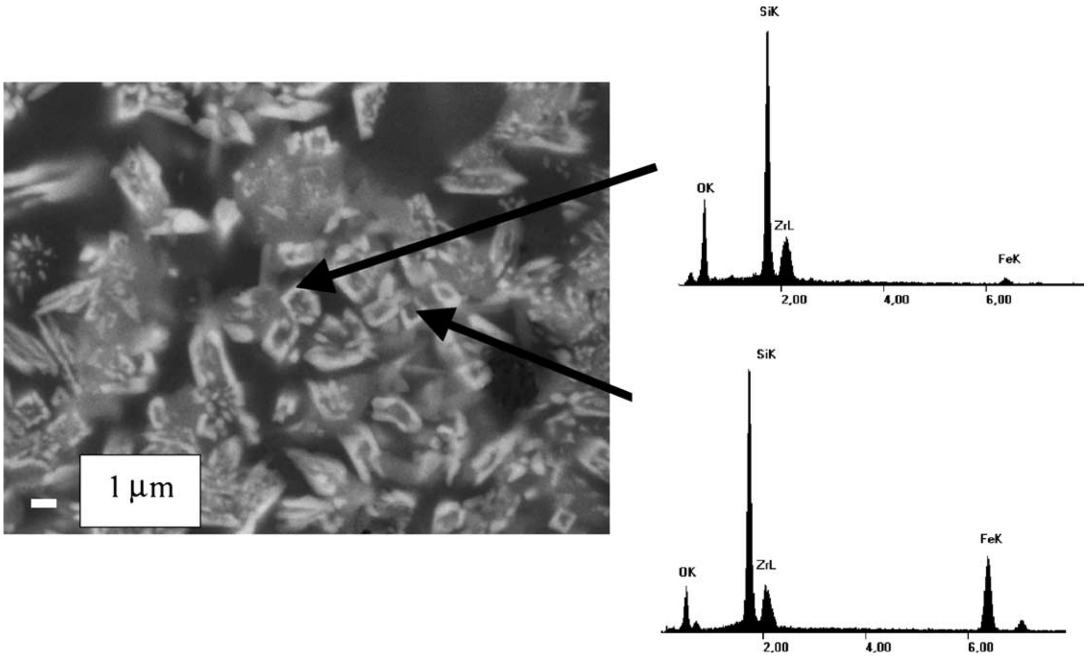

Fig. 10. SEM image of the powdered glass–ceramic pigment (1 h at 850 °C).

in the formed amorphous phase as confirmed by both XRD pattern and SEM micrograph.

In Fig. 11 the a^* values that indicate the predominance of red ($+a^*$) on green ($-a^*$), are reported in comparison with that of an industrial red inclusion pigment (Fe_2O_3–$ZrSiO_4$) commonly used in the ceramic industry. The higher a^* values below 800 °C are to attribute to the "free" hematite present in the samples. As temperature increases, hematite is occluded by the zircon crystallized at the grain boundary, and the a^* value slightly decreases. At 1000 °C an a^* value diminution is due to the solubilization phenomenon of the cromophore ion in the glassy matrix.

Regarding the L^* parameter, which indicates the brightness from $L^* = 0$ black to $L^* = 100$ white, its value increases with increasing temperature. As regarding the heating time effect, longer sintering time (6 and 10 h) do not cause a sensible variation of the color parameters, indicating 1 h as an optimized calcination time.

The CIELab parameters suggest that pigments obtained starting from goethite as iron precursor develop a better red shadow and, moreover, that the color of the glass–ceramic pigment calcined at 800, 850, and 900 °C is comparable with that of the industrial one (similar a^* values).

The analysis of the obtained results suggests a possible mechanism of a glass–ceramic pigment formation based on the sintering and crystallization steps (Fig. 12). After the mixing step the iron precursor is located at the grain boundary of the glassy particles and, during the thermal treatment, as the coalescence of the glassy particles begins at 800 °C, crystalline hematite, both formed in situ from goethite or added in the raw materials mixture, is occluded between the glassy particles. The sintering of the glassy particles is followed by devitrification at the grain boundary that complete the hematite occlusion step through the $ZrSiO_4$ matrix formation.

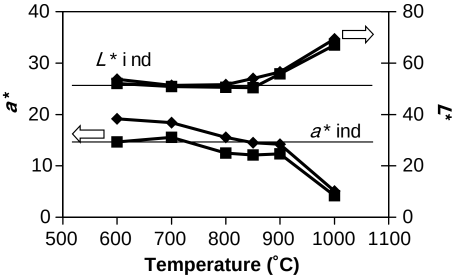

Fig. 11. L^* and a^* values of the glass–ceramic pigments in comparison with the values of an industrial one (bold line); (■) pigments obtained from Fe_2O_3; (▲) pigments obtained from FeOOH.

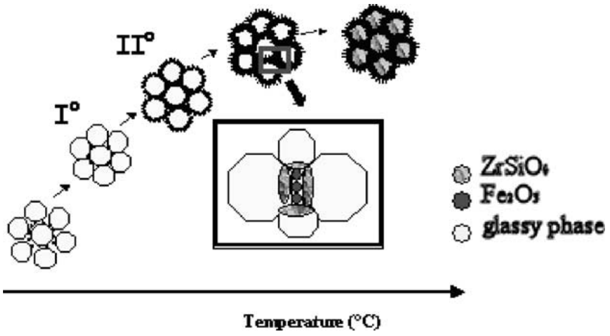

Fig. 12. Occlusion mechanism proposed for the glass–ceramic pigments formation: I° step sintering; II° step crystallization.

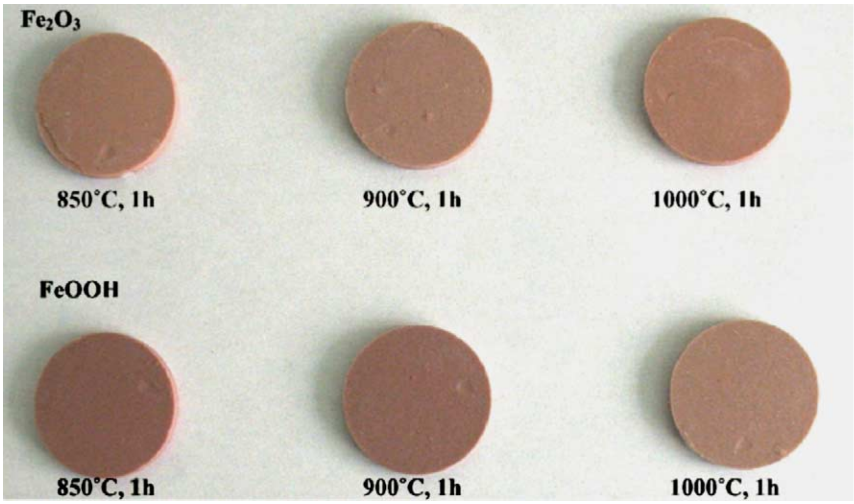

Fig. 13. Red colored porcelained stoneware tiles obtained with the synthesized glass–ceramic pigments.

3.3. Semi-industrial application results

In order to evaluate their coloring capacity, the obtained glass–ceramic pigments calcined at 850, 900, and 1000 °C have been tested in the typical composition of porcelain tile bodies in comparison to both an industrial synthetic coral pink pigment and a natural Grès de Thiviers. No evident changes in water absorption, linear shrinkage, and mechanical and physical properties measured on the fired tile containing different amount of pigments have been observed. It has been determined that addition of Fe_2O_3–Zircon glass–ceramic pigments up to 5 wt.% can be made without modifying the composition of both the body and the industrial process.

With regard to the color of the bodies, all the selected pigments develop a red color (Fig. 13). In Fig. 14 the comparison of the color developed by the glass–ceramic pigments and by both an industrial coral zircon pigment and a natural Grès de Thiviers has been reported. The a^* values measured on the tiles show as the glass–ceramic pigments develop a red color that is less intense of that developed by the industrial coral zircon but is comparable with that exhibited by the natural Grès de Thiviers.

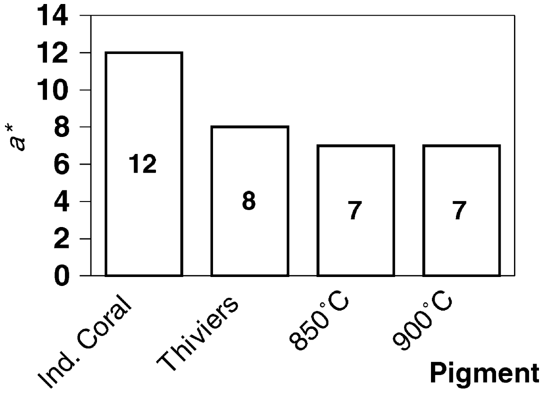

Fig. 14. a^* values of tiles colored by different pigments (2 wt.% in porcelained stoneware bodies).

4. Conclusions

This work has highlighted that it is possible to obtain a zircon-hematite inclusion pigment with an innovative methodology at relatively low temperature. In particular, the mixture containing Li_2O–ZrO_2–SiO_2 glass and FeOOH as iron precursor, heat treated at 850–900 °C for 1 h, develops the best red color similar with that obtained by a natural Grès de Thiviers representing a new possible way to develop a red color in a ceramic body.

Moreover, the obtained results suggest a possible mechanism of pigment formation based on sintering and crystallization steps. These pigments, that we propose to call glass–ceramic pigments, allow to avoid the use of mineralizers and, consequently, the pollutant atmospheric emission such as SO_2, F_2, Cl_2, NO_x frequently present in the gaseous emission of the ceramic pigment productions.

Acknowledgements

Authors are grateful to Dr. Gianni Piergianni who performed the experimental procedure and Dr. Paola Miselli for the assistance in XRD diffraction analysis.

References

1. Eppler, R. A., *J. Am. Ceram. Soc.* 1983, **66**(11), 794.
2. Broll, A., *Keram Z.* 1978, **30**, 324.
3. Kleinchmitt, P., *Keram Z.* 1978, **30**, 688.
4. Lambies, V., *Geoceramics*. Faenza Editrice, Faenza, Italy, 1979.
5. Lambies Lavilla, V. and Rincon Lopez, J. M., *J. Br. Ceram. Soc.* 1981, **80**, 105.

6. Bondioli, F., Ferrari, A. M., Leonelli, C. and Manfredini, T., *Mater. Res. Bull.* 1998, **33**(5), 723.
7. Vicent, J. B., Llusar, M., Badenes, J., Tena, M. A., Vicente, M. and Monros, G., *Bol. Soc. Esp. Ceram.Vidrio* 2000, **39**(1), 83.
8. Dry Colors Manufacturers Association (DCMA). *Classification and chemical description of the mixed metal inorganic colored pigments*. 2nd ed. Washington, DC, USA, 1982.
9. Berry, F. J., Holloway, D. E. J. and Smart, L. E., *J. Mater. Sci.* 1999, **34**, 3631.
10. Llusar, M., Badenes, J. A., Calbo, J., Tena, M. A. and Monròs, G., *Br. Ceram. Trans.* 2000, **99**(1), 14.
11. de Oliveira, A. P. N., Alarcon, O. E., Manfredini, T., Pellacani, G. C. and Siligardi, C., *Phys. Chem. Glasses* 2000, **41**(2), 100.
12. Zanotto, E.D., *Ceram. Trans.*, 1993, 65.